Effect of Polyacrylate Binding Layers on Adhesion of UV-Cured Epoxyacrylate Protective Coatings on Optical Fibers

J. RAYSS,[1] J. WIDOMSKI,[1] I. LUZINOV,[2,*] A. VORONOV,[2,†] S. MINKO[2,‡]

[1] Laboratory of Optical Fibres Technology, Maria Curie-Sklodowska University, 20-031 Lublin, Poland

[2] Lviv Department of Physical Chemistry Institute, Naukova St. 3a, Lviv, 290053, Ukraine

Received 27 February 1997; accepted 12 September 1997

ABSTRACT: Polymer coatings on optical fibers were made of homopolymers of methyl methacrylate, poly(butyl acrylate) and poly(nonyl acrylate), the random copolymer of methyl methacrylate with 5% of methacrylic acid and asymmetric block copolymers of the same acrylates with short polar block of poly(5-*tert*-butyl-peroxy-5-methyl-1-hexen-3-yne-*co*-maleic anhydride) (50 : 50 mol %). They were obtained by means of physisorption of the polymers from the solution on the surface of two sorts of fused silica rods and plates preliminary heated at 200 and 900°C. The contact angle method was employed to evaluate the structure of adsorbed polymer films in the conditions of poor solvent. The fraction of the silica surface capped by the polymer, and surface free energy and its polar and dispersive components were estimated. The results were correlated with the data of adhesion tests between covered silica rods and ultraviolet (UV)-cured epoxyacrylate and discussed in terms of interpenetration of chains of the preliminary adsorbed polymer and polymer matrix. The chains of binding layer (adsorbed polymer) pull-out from the matrix and pull-off from the substrate failure mechanisms were suggested to explain the adhesion data for different sorts of silica rods. The efficiency of the polymer binding layer increases in the following order: asymmetric block copolymer < copolymer < homopolymer. © 1998 John Wiley & Sons, Inc. J Appl Polym Sci **67:** 1913–1923, 1998

Key words: adhesion; polymer connector; failure mechanism; optical fiber

INTRODUCTION

The high-silica optical fibers are used mainly in telecommunication and in medicine as the media transmitting either information or laser energy. Of course, the most important properties of optical fibers are the optical ones, but their mechanical strength is also critical in practical application.

The optical fiber may be considered as a composite material, composed of its inner part, fabricated from high-silica glass (or fused silica), and the outer one, from an organic polymer. The physicochemical parameters of both parts greatly differ. The mechanical properties of such a composite depend on the quality of its glass parts, the properties of polymer coating, and on the phenomena occurring at the glass–polymer interface, especially on the adhesion of polymer protective coatings to the optical fiber surface. It was shown[1] that high adhesion of polymer protective coating

Correspondence to: S. Minko.

* *Present address:* Centre for Education and Research on Macromolecules, University of Liege, Sart-Tilman B6, 4000 Liege, Belgium.

† *Present address:* Institut Charles Sadron, 6 rue Boussingault 67083, Strasbourg, France.

‡ *Present address:* Department of Experimental Physics, University of Ulm, Albert-Einstein-Allee 11, D-89069, Germany.

Journal of Applied Polymer Science, Vol. 67, 1913–1923 (1998)
 CCC 0021-8995/98/111913-11

leads to a decrease of water corrosion of optical fiber, though the process of water permeation through the polymer protective coatings, as well as the phenomenon of rehydroxylation of fused silica surface, are not quite clear.[2,3] On the other hand, it seems, however, that too high adhesion of polymer protective coating may lead to the loss of the energy transmitted, caused by microbendings of the fiber. The reason of the last phenomenon is a great difference of the thermal expansion coefficients of polymer and fused silica.

There are many methods leading to the improvement (or regulation) of adhesion of polymer to solid surfaces. One of them, based on the concept of the interface structure,[4,5] was used in the presented studies of the adhesion of UV-cured epoxyacrylate to the optical fiber's surface.

Theoretical Background

The measured solid–elastomer adhesion or working (or practical[6]) adhesion (G) is usually expressed as[7] follows:

$$G = G_0 + \psi \tag{1}$$

where ψ is the energy dissipated by the material at the crack tip, and (G_0) is the energy of crack growth at zero viscoelastic losses. For elastomeric materials, ψ is considered to be proportional to G_0 and f, where f is a function of the rate of the crack growth, temperature, and deformation value,[8,9] such that

$$\psi = G_0 f \tag{2}$$

and for $f + 1 = \Phi$,

$$G = G_0 \Phi \tag{3}$$

The crack tip fracture energy is multiplied by the Φ function due to the viscoelastic losses in the bulk. In glassy polymers, the situation is more complicated because of the possible plastic deformation in the crack tip. Nevertheless, in many tests at low volume of the loaded material and low rate of a crack growth, the Φ factor is decreased sufficiently. From eq. (3), it is clear that the most fundamental parameter describing adhesion phenomena is G_0, and the effect of polymer interfaces on G_0 is of great interest in numerous investigations. Taking into account a heterogeneous structure of the polymer interface and, consequently, different mechanisms and location of crack formation and growth, G_0 can be expressed as[7] follows:

$$G_0 = iG_0^i + bG_0^b + sG_0^s \tag{4}$$

where G_0^i, G_0^b, and G_0^s is the fracture energy at the interface, in the adhesive layer or the substrate, respectively, and i, b, and s are the fractions of those energies in G_0. Theoretical and experimental investigations of crack propagation on molecular level were performed using tailored polymer interfaces with polymer modificators as the simplest way to control interface properties.[10–14] Grafted polymer chains, block copolymers, or end-functionalized polymers were used as connectors to improve nonpolymer–polymer or polymer–polymer adhesion. It was shown that possible mechanisms of the fracture are pull-out of the connector chains from the polymer, scission of the connector chains, pull-off of the connector chains from the solid substrate, formation of a craze in the polymer adjacent to the interface, and subsequent breakdown of the craze.[15] The addition of the connector significantly increases the interfacial adhesion, and the interfacial fracture energy increases with area density and chain length of the connector. The results were consistent with the model of de Gennes and coworkers,[16,17] as follows:

$$G_0 \approx W + \gamma N \Sigma a^2 \approx W + kTN\Sigma \tag{5}$$

where W is the thermodynamic work of adhesion ($W = \gamma_A + \gamma_B - \gamma_{AB}$), N is the degree of the polymerization of the connector chains, Σ is the area density of the connector chains, γ is the surface energy of the connector chains, and a is the statistical segment length. The measured adhesion energy was found to be a strong function of the rate of crack propagation, even for low speeds of the crack growth when the viscoelastic losses in the bulk were negligible. This fact was explained by a chain pull-out mechanism of the crack propagation. In the case of the crosslinked elastomer, it was found that only portions of long connector chains can be active in enhancing adhesion between elastomers and solids because of the limiting factor of elasticity of the network. The latter limits the penetration of long chains into the elastomer.[13] Authors also considered the possible interaction between the substrate and elastomer that may occur through the connector interlayer due to the chain interpenetrating. Nevertheless,

this phenomena is usually considered insufficient. The latter experiments[13] were performed for the brushes miscible with the polymer of matrix (the same as polymer of matrix). In the case of brushes immiscible with the matrix, we should also consider the effect of interaction parameter (χ) on interface thickness and toughness. Wool[5] argued that the fracture energy for the interface of two immiscible polymers is proportional to interface thickness (d): $G_0 \sim d^2$, while it was predicted[18] that $d = 2a(6\chi)^{-1/2}$. Consequently,

$$G_0 \sim 1/\chi \tag{6}$$

This prediction was derived for the interface between two polymers and does not consider the perturbation introduced by the substrate that takes place in the case of grafted brushes. Experimentally, it was found[19] that d was three times higher than the predicted value.

This short review shows how many factors should be taken into account to tailor the polymer–nonpolymer adhesion. In this work, we consider the effect of the structure of polymer modificators (adsorbed on the substrate) and the morphology of the interface layer on the working adhesion between the fused silica rods and the UV-cured epoxyacrylate. We paid attention on the fact that the liquid oligomer is able to penetrate into the adsorbed polymer layer before hardening and may interact with the silica substrate. Such a heterogeneous structure of the interface could cause the fracture by several mechanisms simultaneously, and fracture energy could be consistent with eq. (4), as it was described recently.[20] It was well documented by Wool[5] that the thermodynamic work of adhesion is substantially lower than the second term in eq. (5), and, consequently, the evaluation of the substrate surface free energy gives nothing to predict the measured adhesion values. Nevertheless, contact angle measurements and surface energy estimation in the case of the polymer covering on solid substrate could be useful for evaluation of the morphology of the polymer film, which effects the adhesion.[20] It was found out that only part of the substrate is capped by the adsorbed polymer film (even formed at adsorption plateau amount), leaving wetting liquid in contact with both the polymer and the surface of the substrate. In order to apply quantitative parameters, the use a model based on the Cassie equation[21] was proposed. According to this model, the surface of a substrate covered by adsorbed polymer film is considered as a planar heterogeneous surface with the following two types of sites: sites where the wetting liquid is in contact with polymer alone, and sites where the liquid is in contact only with the substrate surface, or

$$\cos(\Theta_a) = \eta \cos(\Theta_p) + \varepsilon \cos(\Theta_s), \qquad \eta + \varepsilon = 1 \tag{7}$$

where η is the fraction of the sites screened by polymer; ε is the part of substrate available for the wetting liquid; and Θ_a, Θ_p, and Θ_s are the contact angles for plates covered by adsorbed polymer film, thick polymer films, and uncovered plates with pure surfaces, respectively. In this article, we use this approach to evaluate the morphology of the polymer coatings on the silica substrates and correlate the morphology parameters with adhesion tests.

Nomenclature and Abbreviations

The polymer binding layers formed by physisorbed polymer molecules on the solid substrate, used to tailor the polymer–nonpolymer and polymer–polymer adhesion, are of great interest now and hardly investigated at the molecular scale. That stimulated the development of the new terminology, which is somewhat different from the old widely used technical terms as primer, base coating, or binding layer. In this article, we used such new, becoming commonly used, terms as "connector chains" and "polymer brushes," which, from our point of view, better reflect the peculiarities of the adhesion mechanism of polymers at the molecular level.

ADGD 2.5	composition of two epoxyacrylate resins (see Experimental section)
MMA–MAA	poly(methyl methacrylate-*co*-methacrylic acid)
PBA	poly(butyl acrylate)
PBA–PI	poly(5-*tert*-butyl-peroxy-5-methyl-1-hexen-3-yne-*co*-maleic anhydride)-*graft*-poly(butyl acrylate)
PI	polymer initiator–poly(5-*tert*-butyl-peroxy-5-methyl-1-hexen-3-yne-*co*-maleic anhydride)
PMMA	poly(methyl methacrylate)
PMMA–PI	poly(5-*tert*-butyl-peroxy-5-methyl-1-hexen-3-yne-*co*-maleic anhydride)-*graft*-poly(methyl methacrylate)

PNA	poly(nonyl acrylate)
PNA–PI	poly(5-*tert*-butyl-peroxy-5-methyl-1-hexen-3-yne-*co*-maleic anhydride)-*graft*-poly(nonyl acrylate)
UVCF	UV-curable formulation on the basis of epoxyacrylate ADGD 2.5

EXPERIMENTAL

Materials

Homopolymers of butyl acrylate (PBA), nonyl acrylate (PNA), methyl methacrylate (PMMA), and random copolymer of methyl methacrylate with 5% of methacrylic (MAA) acid (MMA–MAA) were obtained from solution radical polymerization. Polymerization conditions were always such as to ensure approximately the same molecular mass of about 10^5. After synthesis, the polymers were purified by multiple reprecipitation. Purified polymers were used to prepare 0.5% toluene solution. Grafted polymers (PBA–PI, PNA–PI, and PMMA–PI) were obtained by means of radical polymerization in solutions of BA, NA, and MMA, respectively, initiated by polymer initiator (PI)–poly(5-*tert*-butylperoxy-5-methyl-1-hexen-3-yne-*co*-maleic anhydride).[22] The composition of PI was 50 : 50 mol %, with M_n = 2800 and M_w = 3200. The duration of the grafting was calculated to ensure that every molecule of PI initiated the grafting (at least two peroxide groups per PI macromolecule decompose because the efficiency of the initiation reaction is about 0.5), and the molecular weight of the grafted chain is about 10^5. The final product consists of the mixture of homopolymer and grafted polymers of different compositions: one and two grafted chains per molecule of PI (see the scheme in Fig. 1). Grafted copolymers are considered as asymmetric block copolymers since the molecular weight of PI is 30 times lower than the grafted chains. The polarity and, respectively, the adsorption ability of the PI block is higher than that of grafted polyacrylate blocks. The competitive adsorption of asymmetric block copolymers or end-functionalized polymers was investigated, and it was found that short brushes displace long ones[23–25] because of the repulsion of unadsorbed blocks. In the case of adsorption from the mixture of diblock and triblock copolymers (two arm chains grafted to PI), we may predict that the diblock copolymer will displace the triblock copolymer. Thus, in the case of the synthesized mixture, the asymmetric diblock copolymers (PBA–PI, PNA–PI, and PMMA–PI) will be adsorbed preferentially.

The UV-curable formulation (UVCF) was based on the mixture (1 : 1) of two epoxyacrylate resins (ADGD 2.5) synthesized in the Department of Organic Chemistry and Technology, Marie Curie-Sklodowska University, Lublin, Poland, by the esterification of epoxy resins Epidian-2 and Epidian-3 with acrylic acid, as follows:

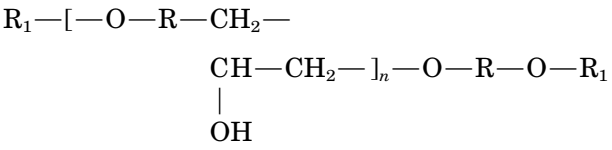

where

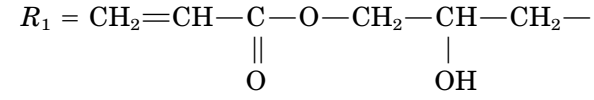

and R equals $-C_6H_4-C(CH_3)_2-C_6H_4-$. 50% of the mixture has $n < 1$ and MM equal to 589, and another fraction has $1 < n < 2$ and MM = 904. UVCF is composed of epoxyacrylate oligomer ADGD 2.5 (75% w/w), active diluent (ethylhexyl acrylate; 23.6% w/w), and photoinitiator (2,2-dimetoxy-2-phenylacetophenone; 1.4% w/w). The properties of the epoxyacrylate composition ADGD 2.5 were previously described in detail.[3,26,27]

For adhesion experiments, 3 mm diameter fused silica rods, freshly drawn in the optical fiber oven from 10 mm preforms (Carl Zeiss, Jena, Germany), or, for the contact angle measurements, fused silica plates (1 × 1 cm, Carl Zeiss, Jena, Germany) were used.

Adsorption Experiments

Two different series of preliminary treated fused silica rods and plates were prepared. The rods and plates were hydroxylated for 12 h in boiling double-distilled water, acidified with hydrochloric acid to pH 3–4. The plates were heated before hydroxylation in air at 600°C in order to remove the organic contamination from their surface. After hydroxylation, the fused silica specimens were washed in double-distilled water, dried in air at 120°C for 1 h, and stored in a dessicator over molecular sieves 4A and 5A. Next, one series of the specimens was heated at 200°C for 12 h, and the second one was heated at 900°C, also for

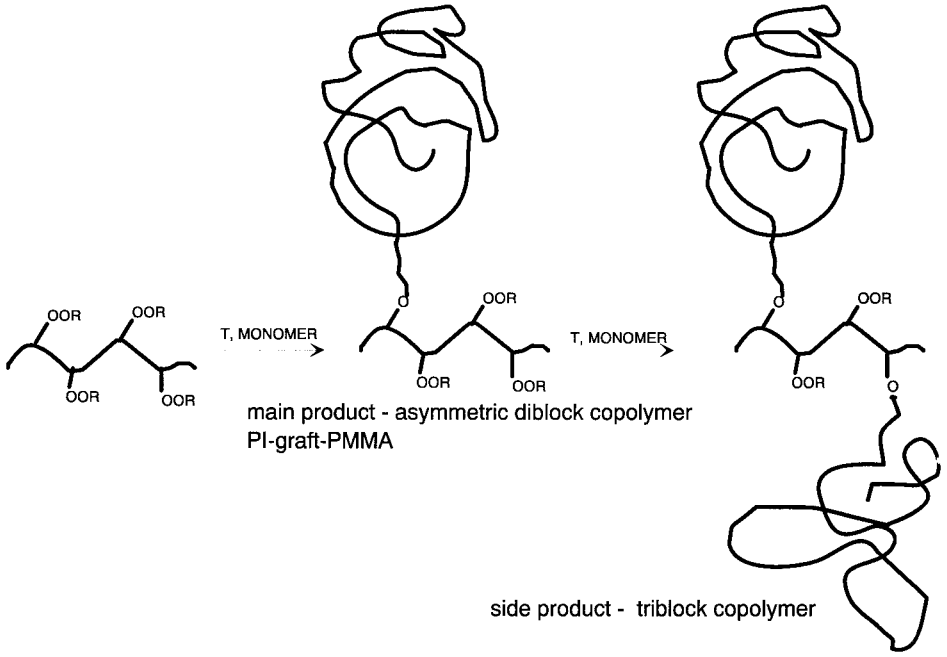

Figure 1 Scheme of the synthesis of asymmetric diblock copolymers.

12 h. We believed, after Zhuravlev,[28] that the silanols concentration on the fully hydroxylated fused silica surface (heated at 200°C) is 4.6 OH/nm,[2] and the one on the surface heated at 900°C is 0.4 OH/nm^2.

The adsorption of polymers was performed by contacting of silica rods and plates with polymer solution (2%) during 6 h. Then, the rods and plates were rinsed six times in toluene and dried at room temperature.

Contact Angle Measurement

The advancing contact angle (Θ) of water, glycerol, foramide, diiodomethane, and UVCF was determined using the sessile drop method. The droplets of liquid were placed on the plates, and the contact angle was measured using a telescope–goniometer constructed in the Laboratory of Optical Fibers Technology (Maria Curie-Sklodowska University of Lublin), with precision $\pm 1°$. The reported results of the contact angle measurements are the average ones, taken from left and right sides of five droplets. Θ for water, diiodomethane, and formamide were measured immediately after the drop was settled. The stability contact angle of liquid UVCF was attained after 5 min of equilibration.

Unbounded thick polymer films (the thickness of these films of 0.1 mm makes it possible to ignore the effect of substrate) were obtained from 10% polymer solution on glass substrates.

Surface free energy (γ_s) and its dispersion (γ_s^d) and polar (γ_s^p) components were calculated by means of the harmonic mean method.[29] This method uses the contact angles of two testing liquids (water and diiodomethane) and is based on the harmonic-mean approach in the Young's equation, as follows:

$$(1 + \cos \Theta_1)\gamma_1 = 4\left(\frac{\gamma_1^d \gamma_s^d}{\gamma_1^d + \gamma_s^d} + \frac{\gamma_1^p \gamma_s^p}{\gamma_1^p + \gamma_s^p}\right),$$

$$(1 + \cos \Theta_2)\gamma_2 = 4\left(\frac{\gamma_2^d \gamma_s^d}{\gamma_2^d + \gamma_s^d} + \frac{\gamma_2^p \gamma_s^p}{\gamma_2^p + \gamma_s^p}\right)$$

where Θ is the contact angle; γ_s^d and γ_s^p are the dispersion and polar components of the surface energy of solid; and the subscripts 1 and 2 refer to the testing liquids 1 and 2, respectively. If γ_j^d and γ_j^p of the testing liquids are known, the dispersion and polar components of solid surface energy can be obtained by solving the two simultaneous equations.

Adhesion Test Method

The specimens for the adhesion measurement were prepared in such a way that the fused silica

Table I Contact Angles (in Degrees) of Glycerol, Water, Formamide, Diiodomethane, and UVCF on the Fused Silica Plates Heated at 200°C and Covered with Adsorbed Polymers

Adsorbed Polymer	Glycerol	Water	Formamide	Diiodomethane	UVCF
Fused silica	38	31	29	34	47.5
PMMA	67	82	56	35	46
PBA	69	79	59	35	55
PNA	91	88	70	53	48
MMA–MAA	66	86	54.5	46	48
MMA–PI	55	52	45	32	51
BA–PI	62	56.5	30	38	50
NA–PI	60	66	42	38	50.5

rods were placed vertically in a polytetrafluoroethylene (PTFE) matrix. Around the rod, a cavity of 10 mm in diameter and 1.2 mm height was milled in the matrix. The cavity was filled with the liquid UVCF formulation. Next, the formulation was cured with UV radiation using a 400-W mercury lamp, while always maintaining the same distance between the lamp and the specimen, equal to 30 cm. The irradiation process (10 min) was carried out in an argon atmosphere. Because the depth of penetration of UV radiation into acrylates is limited to about 300 μm, in order to achieve the complete curing of the polymer ring, the curing process was carried out in the following two stages: after 10 min of irradiation, the fused silica rods with ADGD 2.5 rings were removed from the matrix, and the opposite side of the rings were also cured for 10 min. The additional dose of UV radiation was delivered to the polymer through the fused silica rod, which is transparent for the UV light. After curing, the fused silica rod with a polymer ring was taken from the PTFE matrix, and one end of the rod was placed in the stationary grip of a tensile tester TIRATEST 2200 (Berlin, Germany). The moving grip of the tester was connected by the elastic steel cord with the cone-shaped ring. The cone-shaped ring, placed on the polymer ring, tears the polymer off the surface of the fused silica rod. It was assumed that the adhesion of UVCF to the fused silica surface is equal to the largest strain force registered by the tester, divided by the surface of the polymer ring adhered to the fused silica rod. The results presented in this article are the average taken from 10 measurements. The standard deviation of these measurements was estimated as 1.1% of the average value.

RESULTS

Two series of experiments were performed. In the first series, the surface of silica plates was examined by contact angle measurements. The main aim of this series was to study the structure of adsorbed polymer layers by means of the wetting method. The data of contact angle measurements on fused silica plates covered with adsorbed polymer chains are presented in Tables I and II for plates preliminary heated at 200 and 900°C, respectively. These data were compared with the contact angles of water and UVCF on the thick

Table II Contact Angles (in Degrees) of Glycerol, Water, Formamide, Diiodomethane, and UVCF on the Fused Silica Plates Heated at 900°C and Covered with Adsorbed Polymers

Adsorbed Polymer	Glycerol	Water	Formamide	Diiodomethane	UVCF
Fused silica	53.5	42	33.5	15	64.5
PMMA	70.5	86	69	42	57
PBA	61	59	32	36.5	58
PNA	71.5	84	71.5	40	58
MMA–MAA	75	93	59	43.5	49
MMA–PI	70.5	77	56	38	53
BA–PI	72.5	69	60	38	52.5
NA–PI	70	61.5	40	32	50.5

Table III Contact Angles of Water and UVCF on Thick Polymer Films

Polymer Film	Contact Angle of Water (Degree)	Contact Angle of UVCF (Degree)
PMMA	76	57.5
PBA	91	52.5
PNA	99	49
MMA–MAA	80	40.5

polymer films of the polymers, shown in Table III. In many cases, the contact angles of water and UVCF on the unbounded film are higher than those on the plates covered by adsorbed film. The reasons for this behavior were discussed in the Introduction of this article with the aim of eq. (7). Equation (7) is valid if the wetting of the polymer chain in adsorbed layer and thick polymer film is the same, or, otherwise, the same fraction of polar groups is exposed outwardly (available for wetting liquid) of the adsorbed polymer chain and thick polymer film. In the case of adsorbed diblock copolymers, it is uncertain that the polar fragment (anhydride groups of PI blocks) orientation is the same in the thick film and on the substrate because of the selective adsorption of one block on the silica substrate. Nevertheless, for homopolymers and random copolymers, eq. (7) could be considered if the segment–segment and segment–surface site (of the substrate) interactions are close.[30] Thus, we used eq. (7) for the calculation of η only for the homopolymers and copolymer (Tables IV and V). Table I shows that the magnitudes of Θ_a and Θ_p measured by UVCF are very close for the plates heated at 200°C and cannot be used for the calculation of η. Only η values measured with water are presented in Table IV. The data of Tables I and II were used to calculate the surface free energy (γ_s) and its polar (γ_s^p) and dispersive (γ_s^d) components (Tables IV and V) by means of the harmonic mean method.

In the second series of experiments, the adhesion tests were performed using the rods with different adsorbed polymer layers. The data are presented in Tables IV and V.

DISCUSSION

It is evident from the results presented in Tables IV and V that all polymer binding layers used decrease the adhesion strength, with one exception for the PMMA coating on the fused silica rods heated at 900°C. The weak connector chains–silica or connector chains–matrix interactions are possible reasons for the results. The interlayer structure plays the main role in those interactions. The connector–silica substrate interaction depends on the energy of connector–surface site interaction and the concentration of hydroxyl groups on the silica surface. The connector–matrix interaction depends on the adsorbed chain conformation, as follows: fraction of polymer in loops and tails, and length of loops and tails (for adsorbed homopolymers and copolymer); grafting chain area concentration, and length of grafted chains (for grafted brushes); χ parameter of the connector chain–matrix interaction; fraction of the surface capped by the connector; and space between crosslinks in the matrix. Numerous parameters influence the adhesion and make it very difficult to clarify all aspects of the behavior;

Table IV Adhesion of Cured UVCF to Fused Silica Rods Heated at 200°C, η Parameter (Determined from Water Contact Angle), and Surface Free Energy γ_s and Its Polar γ_s^p and Dispersive γ_s^d Components of the Fused Silica Plates Heated at 200°C and Covered with Different Polymers

Adsorbed Polymer	Adhesion (N/mm^2)	η	γ_s (mJ/m^2)	γ_s^p (mJ/m^2)	γ_s^d (mJ/m^2)
Fused silica	8.13	0	86.1	45.1	41.0
PMMA	7.03	1.16	49.8	9.2	40.6
PBA	6.52	0.76	51.5	10.8	40.6
PNA	6.04	0.81	40.2	7.8	32.4
MMA–PI	6.49	—	70.4	28.7	41.7
BA–PI	6.44	—	65.3	26.03	39.3
NA–PI	5.56	—	58.5	19.2	39.3
MMA–MAA	6.61	1.15	43.8	8.1	35.8

Table V Adhesion of Cured UVCF to Fused Silica Rods Heated at 900°C, η Parameter (Determined from Water and UVCF Contact Angles), and Surface Free Energy γ_s and Its Polar γ_s^p and Dispersive γ_s^d Components of the Fused Silica Plates Heated at 900°C Covered with Different Polymers

Adsorbed Polymer	Adhesion (N/mm^2)	η[a]	γ_s (mJ/m^2)	γ_s^p (mJ/m^2)	γ_s^d (mJ/m^2)
Fused silica	7.22	0	8.18	34.8	47.0
PMMA	7.93	1.35/1.07	45.3	7.7	37.6
PBA	6.18	0.30/0.55	41.9	2.0	39.9
PNA	5.46	0.71/0.44	46.5	8.5	38.0
MMA–PI	5.33		51.5	12.2	39.3
BA–PI	5.33		56.5	17.2	39.3
NA–PI	5.54		63.5	21.7	41.8
MMA–MAA	6.28	1.40/0.68	41.1	4.4	37.0

[a] Numerator, by water; denominator, by UVCF.

hence, in this article, we attempt to discuss the role of some of them.

First of all, we discuss the connector layer structure estimated by contact angle measurements. The silica surface is capped by adsorbed polymer to a considerable extent (Tables IV and V). Values of $\eta > 1$ for PMMA and MMA–MAA show that eq. (7) is not valid. In this case, the distribution of polar sites in the adsorbed chain differs from that of the thick polymer film. The polar sites are directed to the silica surface. This is an evidence of the strong connector–substrate interaction in the case of these polymers. In the case of other homopolymers, the data prove that some fraction of the surface is not capped by connector chains. The ester group of acrylic or methacrylic acid is responsible for the polyacrylate–silica substrate interaction. Thus, the energy of connector segment–substrate interaction should be the same for all homopolymers, but big alkyl substitutes in PBA and PNA blocks change the orientation of polar segments, and, in contrast to PMMA, for these polymers, $\eta < 1$. It is interesting that in most cases, η values estimated with UVCF are lower than those with water. Consequently, UVCF somewhat rearranges the connector layer because it is a better solvent for the polymers than water.

For all silica plates covered with polymers, γ_s is lower than for the pure silica surface. The surface free energy of pure silica consists of two approximately equal polar and dispersive components for the plate heated at 200°C; for the plate heated at 900°C, the dispersive component is larger because of decreased concentration of hydroxyl groups on the surface. For the plates covered by homopolymers and the MMA–MAA copolymer, we obtained similar γ_s values for both kinds of plates, heated at 200 and 900°C. Besides, the dispersive components are substantially larger than the polar components, but, in most cases, the polar component for plates heated at 200°C is larger than that for plates heated at 900°C. Those facts prove that the surface of plates is capped by the polymer to a great extent, and the surface free energy is influenced mainly by the dispersive component. There is no pronounced difference of the surface free energies in the series of homopolymers with various alkyl substitutes.

For the plates covered by the grafted polymers, the effect of the monomer nature is pronounced substantially. In the range of block copolymers with the blocks MMA, BA, and NA brushes, γ_s decreases for plates heated at 200°C and increases for plates heated at 900°C. The polar component of the surface free energy changes in the same way, and the magnitude of the polar component is larger than in the case of the homopolymers. The latter is evidence of the fact that wetting liquid penetrates through a brush layer better than for adsorbed homopolymer or copolymer layers. Such behavior of the polymer brushes could be explained by their specific features in a poor solvent or in air. The polymer brushes in such layers were analyzed in theoretical works and studied experimentally.[31–33] It was found that for sufficiently poor solvents, the laterally homogeneous grafted layer is linearly unstable to fluctuations tangential to the grafting plane and forms a dimpled surface in which the depth and separation of the dimples

Table VI Conclusions About the Failure Mechanisms

Silica Substrate	Adsorbed Polymer	Data	Failure Mechanism
Heated at 200°C	PMMA–PI PBA–PI PNA–PI	Adhesion is sensitive to the compatibility of the adsorbed polymer with the matrix and the fraction of the capped substrate surface	Pull-out of the polymer modificator chains from the matrix
	PMMA PBA PNA MMA–MAA	Adhesion is sensitive to the compatibility of the adsorbed polymer with the matrix and insensitive to γ_s	Pull-out of the polymer modificator chains from the matrix
Heated at 900°C	PMMA–PI PBA–PI PNA–PI	Adhesion is sensitive to the concentration of hydroxyl groups on the substrate surface and insensitive to the structure of the adsorbed layer	Pull-off from the silica substrate

depends on chain length, solvent quality, and grafting density. This instability is caused by the competition between the attractive forces between chains and the grafting constraints. Consequently, the high permeability of the grafted layers can be caused by a dimpled structure. The larger the alkyl substitute, the lower the permeability that is observed for plates heated at 200°C. For the plates heated at 900°C, we obtained the reverse relationship. Obviously, the lower energy of interaction of the dehydroxylated silica surface with anchor chains of the grafted polymer allows the grafted layer more possibilities to be rearranged (for example, to move along the surface or force out some amount of the polymer from the substrate).

Thus, we have some information about the structure of the polymer binding layers in a poor solvent, we assume that the layers have similar structure after the contact with the matrix polymer, and now we can discuss the data of adhesion tests (Tables IV and V). For grafted polymer layers, the adhesion values for the rods heated at 900°C are the same for all different brushes and lower than that for the rods heated at 200°C. Only for NA–PI grafted block copolymer, adhesion is the same for both sorts of silica plates. We may presume from these data that for the rods heated at 900°C, the failure mechanism is pull-off PI anchors from silica substrate.

In the case of homopolymer connectors, the level of adhesion is the same for both sorts of plates, and there is no relationship between adhesion and γ_s values; but the larger the alkyl substitute, the lower the adhesion that is observed. Consequently, we may assume that, in this case, the failure mechanism is pull-out of polyacrylate blocks from the matrix, and the adhesion strongly depends on the compatibility parameter [eq. (6)]. From the general consideration, we can conclude that the compatibility in the polyacrylate–epoxyacrylate matrix system decreases with increasing size of alkyl substitute of the polyacrylate. Consequently, the decrease of adhesion in the series PMMA, PBA, and PNA is caused by the decrease of compatibility with matrix, and there is no pronounced effect of the fraction of capped surface. The same inferences about the pull-out mechanism can be drawn for grafted chains on the rods heated at 200°C, while the decrease of adhesion in the range MMA–PI, BA–PI, and NA–PI can be explained by the following two reasons: the decrease of compatibility of polyacrylates with the matrix, and the decrease of the fraction of capped silica surface.

It is interesting to compare the adhesion strength in the series of polymer modificators, PMMA, MMA–MAA, and MMA–PI. The adhesion decreases in this series for both sorts of the rods. One can see again that there is no relationship between measured adhesion and surface free energy. The structures of adsorbed layers of PMMA and MMA–MAA must be very close because of the small fraction of MAA units in the copolymer. MAA units improve the connector–substrate interaction, but adhesion decreases in the case of MMA–MAA. Consequently, the adhesion is influenced by the chain pull-out mechanism of PMMA loops and tails from the matrix. Taking into account the equal molecular weight

of MMA–MI, PMMA polymers, and PMMA blocks in MMA–PI, it is clear that the length of PMMA chains penetrated into the matrix decreases in the series MMA–PI, PMMA, and MMA–MAA. Since poly–MMA segments do not form any bonds with the substrate, in the case of MMA–PI the maximum amount of such bonds, the MMA–MAA copolymer should form by means of MAA fragments. Because of the small fraction of MAA fragments, the difference between MMA–MAA and PMMA is expected to be small.[34] If we accept the idea of optimal length of the active connector for adhesion to the crosslinked matrix (the interpenetrating of a brush and network is controlled by spacing between crosslinks) suggested in the recent work,[13] we can assume that the PMMA adsorbed layer could be closer to optimal length of loops and tails because of its flexibility to adjust the conformation: there are no blocks or segments adhered to the substrate more strongly than other segments. Such flexibility is higher when the segment–substrate interaction is lower. Possibly, this is the reason that for the PMMA connector, adhesion is higher for the rods heated at 900°C. This is the only sample in the investigated series in which the polymer connector enhanced adhesion against the uncovered silica surface. Obviously, the homopolymer that is compatible with the matrix and has higher adhesion to the substrate is the best modificator to improve nonpolymer–crosslinked polymer adhesion. The conclusions about failure mechanisms are summarized in Table VI.

CONCLUSIONS

The contact angle method is useful for evaluation of the structure of dry adsorbed polymer films or films in conditions of a poor solvent on the surface of a solid substrate. That evaluation can be applied for the analysis of the adhesion data between the substrate covered by the layer of polymer connector and a polymer matrix in terms of interpenetration. The data obtained for polyacrylate connectors of different structure on the surface of fused silica suggest that dehydroxylation of the silica surface changes the failure mechanism from pull-out of the connector chains from epoxyacrylate matrix (in the case of the silica surface heated at 200°C) to pull-off of the connector from silica surface (heated at 900°C). For the pull-out mechanism, the length of the connector chain and its compatibility with the matrix play the most important role in the adhesion. The efficiency of the polymer connectors increases in the following series: grafted brushes < copolymer < homopolymer. At a low concentration of the hydroxyl groups on the substrate surface, the physisorbed grafted polymers have poor adhesion to the substrate and cause the failure. The homopolymer adsorbed layer can easier rearrange the structure to optimize the both interactions, polymer modificator–substrate and polymer modificator–matrix, and improve the adhesion. The results obtained can be used for the choice of appropriate connectors to improve fused silica-cured epoxyacrylate adhesion.

REFERENCES

1. C. R. Kurkijan and D. Innis, *Opt. Eng.,* **30,** 681 (1991).
2. J. Rayss, J. Widomski, and W. M. Podkoscielny, *Optoelectr. Rev.,* **3,** 107 (1995).
3. J. Rayss, W. M. Podkoscielny, A. Walewski, *Proc. SPIE,* **1085,** 288 (1989).
4. L. T. Drzal, *Adv. Polym. Sci.,* **75,** 1 (1985).
5. R. P. Wool, *Polymer Interfaces: Structure and Strength,* Hanser, Munich, 1995.
6. K. L. Mittal, *Adhesion Measurements of Films and Coatings,* K. L. Mittal, Ed., VSP, Zeist, 1995, pp. 1–13.
7. A. J. Kinloch, *Adhesion and Adhesives. Science and Technology,* Chapman and Hall, London, 1987.
8. E. H. Andrews, A. J. Kinloch, *Proc. R. Soc., London,* **A332,** 385 (1973).
9. A. N. Gent, I. J. Schultz, *Adhesion,* **3,** 281 (1972).
10. H. R. Brown, *Macromolecules,* **26,** 1666 (1993).
11. H. R. Brown, *Annu. Rev. Mater. Sci.,* **21,** 463 (1991).
12. A. Halperin, M. Tirell, T. P. Lodge, *Adv. Polym. Sci.,* **31,** 100 (1992).
13. M. Deruelle, L. Leger, M. Tirell, *Macromolecules,* **28,** 7419 (1995).
14. C. F. Creton, E. J. Kramer, H. Hui, H. R. Brown, *Macromolecules,* **25,** 3075 (1992).
15. J. S. Swith, E. J. Kramer, P. J. Mills, *J. Polym. Sci., Polym. Phys.,* **32,** 1731 (1994).
16. E. Raphael, P.-G. de Gennes, *J. Phys. Chem.,* **96,** 4002 (1992).
17. H. Ji, P.-G. de Gennes, *Macromolecules,* **26,** 520 (1993).
18. E. Helfand, Y. Tagami, *J. Chem. Phys.,* **56,** 3592 (1971).
19. C. J. Clarke, R. A. L. Jones, J. L. Edwards, K. R. Shull, J. Penford, *Macromolecules,* **28,** 2042 (1995).
20. I. Luzinov, A. Voronov, S. Minko, *Adsorp. Sci. Technol.,* **14,** 259 (1996).

21. A. B. D. Cassie, S. Baxter, *Trans. Faradey Soc.,* **40,** 546 (1944).
22. V. S. Kurgansky, V. A. Puchin, S. A. Voronov, V. S. Tokarev, *Vysokomol. Soedin. Seria A,* **25,** 997 (1983) (transl. to English).
23. J. Klein, Y. Kamiyama, H. Yoshizawa, J. N. Israelachvili, L. J. Fetters, P. Pincus, *Macromolecules,* **25,** 2062 (1992).
24. E. Kumacheva, J. Klein, P. Pincus, L. J. Fetters, *Macromolecules,* **26,** 6477 (1993).
25. D. F. Siqueira, J. Reiter, U. Breiner, R. Stadler, M. Stamm, *Langmuir,* **12,** 972 (1996).
26. J. Rayss, W. M. Podkoscielny, J. Widomski, A. Gorgol, *J. Appl. Polym. Sci.,* **53,** 1833 (1994).
27. J. Rayss, W. M. Podkoscielny, J. Widomski, *J. Appl. Polym. Sci.,* **49,** 835 (1993).
28. L. T. Zhuravlev, *Colloids Surf. A.,* **74,** 835 (1993).
29. S. Wu, *Polymer Interface and Adhesion,* Marcel Dekker, New York, 1982.
30. S. S. Minko, I. A. Luzinov, A. S. Voronov, *Colloid J.,* **56,** 720 (1994).
31. C. Yeung, A. C. Balazs, D. Jasnow, *Macromolecules,* **26,** 1914 (1993).
32. H. Tang, I. Szleifer, *Europhys. Lett.,* **28,** 19 (1994).
33. D. F. Siqueira, K. Köhler, M. Stamm, *Langmuir,* **11,** 3092 (1995).
34. B. van Lent, J. M. H. M. Scheutjens, *J. Phys. Chem.,* **94,** 5033 (1990).